Drug Development and Industrial Pharmacy

ISSN: 0363-9045 (Print) 1520-5762 (Online) Journal homepage: http://www.tandfonline.com/loi/iddi20

Self-dispersible nanocrystals of albendazole produced by high pressure homogenization and spray-drying

Alejandro Javier Paredes, Juan Manuel Llabot, Sergio Sánchez Bruni, Daniel Allemandi & Santiago Daniel Palma

To cite this article: Alejandro Javier Paredes, Juan Manuel Llabot, Sergio Sánchez Bruni, Daniel Allemandi & Santiago Daniel Palma (2016) Self-dispersible nanocrystals of albendazole produced by high pressure homogenization and spray-drying, Drug Development and Industrial Pharmacy, 42:10, 1564-1570, DOI: 10.3109/03639045.2016.1151036

To link to this article: http://dx.doi.org/10.3109/03639045.2016.1151036

Accepted author version posted online: 09 Feb 2016.
Published online: 08 Mar 2016.

DRUG DEVELOPMENT AND INDUSTRIAL PHARMACY, 2016
VOL. 42, NO. 10, 1564–1570
http://dx.doi.org/10.3109/03639045.2016.1151036

Taylor & Francis
Taylor & Francis Group

RESEARCH ARTICLE

Self-dispersible nanocrystals of albendazole produced by high pressure homogenization and spray-drying

Alejandro Javier Paredes[a,b], Juan Manuel Llabot[a,b], Sergio Sánchez Bruni[c], Daniel Allemandi[a,b] and Santiago Daniel Palma[a,b]

[a]Unidad de Investigación y Desarrollo en Tecnología Farmacéutica, UNITEFA (CONICET), Córdoba, Argentina; [b]Departamento de Farmacia, Facultad de Ciencias Químicas, Universidad Nacional de Córdoba, Córdoba, Argentina; [c]Laboratorio de Farmacología, Facultad de Ciencias Veterinarias, CIVETAN (CONICET), Universidad del Centro de la Provincia de Buenos Aires, Campus Universitario, Tandil, Buenos Aires, Argentina

ABSTRACT

Albendazole (ABZ) is a broad-spectrum antiparasitic drug used in the treatment of human or animal infections. Although ABZ has shown a high efficacy for repeated doses in monogastric mammals, its low aqueous solubility leads to erratic bioavailability. The aim of this work was to optimize a procedure in order to obtain ABZ self-dispersible nanocrystals (SDNC) by combining high pressure homogenization (HPH) and spray-drying (SD). The material thus obtained was characterized and the variables affecting both the HPH and SD processes were studied. As expected, the homogenizing pressure and number of cycles influenced the final particle size, while the stabilizer concentration had a strong impact on SD output and redispersion of powders upon contact with water. ABZ SDNC were successfully obtained with high process yield and redispersibility. The characteristic peaks of ABZ were clearly identified in the X-ray patterns of the processed samples. A noticeable increase in the dissolution rate was observed in the aqueous environment.

ARTICLE HISTORY
Received 17 November 2015
Revised 26 December 2015
Accepted 19 January 2016
Published online 7 March 2016

KEYWORDS
Albendazole; enhanced dissolution rate; high pressure homogenization; nanocrystals; pluronic 188; poloxamer 188; poor solubility; spray drying

Introduction

The poor permeability or solubility of some drugs can be limiting conditions for oral absorption, leading to a consequent decrease in bioavailability. ABZ, methyl [5-(propylthio)-1-H-benzimidazol-2yl] carbamate, a benzimidazole with a broad-spectrum antiparasitic effect, acts by preventing the polymerization of microtubules in eukaryotic cells[1]. Although ABZ has shown a high efficacy, its low aqueous solubility results in erratic oral bioavailability[2]. ABZ is a class II drug in the Biopharmaceutics Classification System[3,4], which implies low solubility/high permeability, with these features having been linked to therapeutic failures following oral administration of ABZ[5]. For class II drugs, an improvement in solubility can also lead to an increase in bioavailability. However, permeability is an intrinsic drug property that is difficult to modify, with different strategies having been developed which can improve ABZ water solubility and dissolution rate, such as the formulation of solid dispersions[6], oil/water emulsion[7], incorporation into liposomes[8], complexation with cyclodextrins[9], co-grinding[10] and the synthesis of new analogs with higher solubility[11,12].

Increased systemic bioavailability of ABZ has also been reported when the drug was co-administered with fatty meal[13], fruit juice[14], cosolvent[15] or surfactants[16]. In addition, several clinical studies have demonstrated that an enhanced systemic availability of the parent drug/active metabolite obtained by increased drug absorption correlates with an improved antiparasitic effect[7,8,15,17–22]. Nevertheless, most of strategies described above have had only limited success in the improvement of ABZ bioavailability, with the methods proposed being in general difficult to scale up for industrial production. Thus, there arises the need to find a simple, efficient and scalable method to produce new ABZ formulations with increased bioavailability. Bearing this in mind, the formulation of ABZ nanocrystals (NC) appears to be a useful tool to achieve this goal, since it is possible to obtain particles with sizes below 1μm and the ability to redisperse in aqueous environments. The key feature of NC is its enlarged surface area, which leads to a faster saturation in the dissolution layer around the particles with a consequent increase in dissolution rate, according to the Noyes-Whitney equation[23,24]. These advantages, in addition to formulation simplicity and ease of scale up, has caught the attention of the pharmaceutical industry, which is reflected in six licensed drug products being launched in the market and another four undergoing pre-clinical stage studies[25].

"Bottom-up" and "top-down" techniques are the processes used for nanocrystal manufacture. HPH is a top-down technique in which the drug suspension passes through a very thin gap at an extremely high velocity, producing cavitation phenomena and consequent particle breaking[23]. After nanonization, water elimination is required, with the most commonly used methods being lyophilization and SD. The former is costly and time consuming, while the latter is a rapid and convenient method[26]. The main challenge in SD of nanosuspensions is the attainment of a product with high yield (>60%) and a powder able to be easily redispersed into nanosized particles upon contact with water.

The aim of this work was to obtain self-dispersible ABZ nanocrystals from an optimized process whose main steps involved the comminution of ABZ by HPH technology in order to obtain an aqueous nanosized suspension, with further water removal being achieved by SD.

CONTACT Santiago Daniel Palma sdpalma@fcq.unc.edu.ar Unidad de Investigación y Desarrollo en Tecnología Farmacéutica, UNITEFA (UNC-CONICET); Departamento de Farmacia, Facultad de Ciencias Químicas, Universidad Nacional de Córdoba, Córdoba, Argentina

Materials and methods

Materials

Albendazole USP grade and Sodium dodecyl sulfate (SDS) were purchased from Todo Droga, Argentina and the stabilizers Poloxamer 188 (P188) and Poloxamer 407 (P407) were obtained from RUMAPEL, Argentina. Mannitol, lactose and other reagents were of pharmaceutical grade.

Physical mixture

For the solubility assay, X-ray diffraction of powders and dissolution assay, a physical mixture (PM) of ABZ, P188 and lactose was used as control. This was prepared in an Agatha mortar using the same composition of SDNC (SD_4) as shown in Table 2.

Preparation of Albendazole nanosuspensions

Different formulations of ABZ nanocrystal suspensions were prepared by varying the type and amount of stabilizers (SDS, P407 or P188), while keeping the amount of ABZ fixed. Accurately weighed ABZ and one of the excipients were ground in a mortar, and deionized water was gradually added until a homogeneous suspension was obtained. Afterwards, the suspension was transferred to a beaker and sonicated for five minutes. A pre-milling process of 3 cycles at 500 bar was performed for all runs to protect the homogenizer check valves from blocking. Then, 30 and 20 cycles (NS_{1-3} and NS_{4-7}, respectively) of high pressure homogenization at 1200 bar (Avestin C5 Emulsiflex®; Avestin Inc., Ontario, Canada) were applied. NS_{4-7} were also processed at 1000 bar to evaluate the effect of the homogenization pressure and stabilizer concentration. Samples were cooled using a heat exchanger with counter-flow cold water (5 °C) during the homogenization process. The batch size was 100 g in all cases, with the formulation composition and homogenization parameters being depicted in Table 1.

Preparation of SDNC by spray-drying

The SD process was performed on a laboratory-scale Mini Spray-dryer Büchi B-290 (Büchi Labortechnik, AG Flawil, Switzerland) equipped with a dehumidifier module. Technical data and the scheme of the drying apparatus can be found at the manufacturer's web site. A two-fluid nozzle with a cap orifice diameter of 1.5 mm was used, and the operating conditions were: atomization air (L/h): 819, aspiration (m^3/h): 30, temperature (°C): 45 and pump (ml/min): Anhydrous lactose was used as a supporting agent at increasing lactose:ABZ mass ratios (0, 1:6 and 1:3), as shown in Table 2. After being added, the suspension was stirred for 10 min before drying. In order to maintain sample homogeneity, slow magnetic stirring was kept constant during the drying process.

Eventual particle aggregation post-HPH and pre-drying was discarded by measuring particle size and PI of the nanosuspensions (NS_4–NS_7) at room temperature for 7 days. The powders obtained by SD were evaluated by measuring particle size, polidispersity index (PI), process yield and moisture content.

Table 1. Composition and operating conditions of ABZ nanocrystal suspensions obtained by HPH.

Formulation	ABZ (g)	SDS (g)	P407 (g)	P188 (g)	Water (mL)	Cycles-Pressure (bar)
NS_1	2.5	2.5	–	–	95	30-1200
NS_2	2.5	–	2.5	–	95	30-1200
NS_3	2.5	–	–	2.5	95	30-1200
NS_4*	2.5	–	–	0.25	97.25	20-1200
NS_5*	2.5	–	–	0.5	97	20-1200
NS_6*	2.5	–		1	96.5	20-1200
NS_7*	2.5	–	–	2.5	95	20-1200

*These samples were also processed at 1000 bar to evaluate the effect of pressure and P188 concentration on the reduction of particle size.

Table 2. Spray-dried powder obtained from ABZ nanocrystal suspensions produced by HPH.

Formulation	ABZ (g)	P188 (g)	MiliQ Water (mL)	Lactose:ABZ
SD_1	2.5	0.25	97.25	1:6
SD_2	2.5	0.5	97.00	1:6
SD_3	2.5	1	96.50	1:6
SD_4	2.5	2.5	95.00	1:6
SD_5	2.5	2.5	95.00	1:3
SD_6	2.5	2.5	95.00	0

Lactose:ABZ is expressed as a mass ratio. Powders SD_{1-4} were obtained from NS_{4-7}, respectively. SD_{5-6} were obtained from NS_7 by varying the amount of lactose.

Characterization

Particle size and PI measurement

The particle size and PI values of ABZ nanocrystal suspensions and the redispersed samples were determined by Photon Correlation Spectroscopy (Delsa™ Nano C Particle Analyzer, Beckman and Coulter, Inc., Pasadena, CA). Before taking measurements, samples were diluted with deionized water in order to obtain the required absorption intensity. For this purpose, ~20 mg of powder was added to 5 ml of water, and the resultant suspension was shaken by hand for 1 min before carrying out the assays.

Microscopy

Scanning electron microscopy Images of pure ABZ, nanosuspension (NS_7), SDNC (SD_4) and the corresponding redispersed nanocrystals were taken by scanning electron microscopy (SEM). To carry this out, powders (ABZ and SD_4) and a drop of nanosuspension or redispersed SDNC were placed on aluminum studs. NS_7 and its redispersed sample were dried at 30 °C in an oven. Then, samples were sputtered with Au before examination using a Scanning Electron Microscope (ZEIZZ, Oberkochen, Germany).

Optical microscopy The original nanosupension NS_7 and the redispersed nanocrystals SD_4 were analyzed in a Light Microscope (Olympus BX41; Olympus Latin America Inc., Miami, FL) equipped with an Infinity® 1 camera (Olympus Latin America Inc., Miami, FL) at 40×.

Moisture content

The powder moisture content was measured immediately after the spray-drying step in a moisture analyzer with halogen heating (OHAUS M45®, Parsippany, NJ).

Solubility assay

Excess amounts of pure ABZ, PM and spray-dried nanocrystals (SD_4) were placed in hermetic screw cap tubes, before adding 5 ml of deionized water or HCl 0.1 N. The hermetic tubes were then transferred to a thermostatic bath (Vicking Dubnoff®; Vicking SRL, Buenos Aires, Argentina) at 25 °C equipped with a mechanical shaker tray. After 48 h, 2 ml of suspension were withdrawn and centrifuged at 10 000 rpm. The supernatants were filtered through a Millipore 0.22 µm membrane filter and quantified by means of a U.V. spectroscopy at 299 nm (Thermo

Evolution 300, Waltham, MA). All samples were analyzed in triplicate.

Powder X-ray diffraction

X-ray diffraction patterns were obtained to assess the crystallinity of ABZ, PM and the spray-dried nanocrystals (SD_4). For this purpose, powders were analyzed in a PANalytical X-Pert Pro® X-ray powder diffractometer (PANalytical B.V., Almelo, Netherlands) with Cu-Kα radiation, between 5° and 50° in 2θ in steps of 0.04, and counting time at 0.5 s per step.

Dissolution assay

Dissolution tests of pure ABZ, PM and SDNC placed in transparent hard gelatine capsules were performed using a USP XXIV dissolution apparatus 1 (SOTAX AT 7 Smart; SOTAX Corporation, Westborough, MA). The rotational basket speed was set at 75 rpm, and the temperature kept constant at 37 ± 0.5 °C. The assayed amount of ABZ was 200 mg in all experiments. For the dissolution medium, 900 ml 0.1 N HCl was used. Five-milliliter aliquots were withdrawn at predetermined time intervals over 2 h with reposition of fresh medium. Samples were filtered, and the concentration of dissolved drug was measured at 299 nm using a UV–Vis spectrophotometer (Thermo Evolution 300, Waltman, MA). All dissolution assays were performed in triplicate.

In previous test, we verified that the presence of carriers dissolved in the dissolution medium did not affect the λ_{max} of ABZ. The percentages of dissolved drug were statistically analyzed by one-way analysis of variance. The differences were considered statistically significant at $p < 0.05$.

Results and discussion

Particle size of nanosuspensions

Although the principal parameters affecting the final particle size in HPH have been previously reported to be temperature, number of homogenizing cycles and power density of the homogenizer[23], in the present study, the influence of the stabilizer type (SDS, P407 or P188) at fixed processing conditions was evaluated as shown in Figure 1. The presence of different additives did not appear to affect the way in which ABZ crystals decreased in size, since for different amounts of homogenizing cycles the samples revealed similar particle sizes (i.e. at 20 cycles, NS_1: 523 nm, NS_2: 519 nm and NS_3: 522 nm), with PI values being between 0.35 and 0.25 after 10 homogenizing cycles in all cases. Moreover, no variations in particle size were observed after 20 cycles, with this phenomenon being previously explained as resulting from the exhaustion of weak points in the particle, which impedes new fractures after a certain number of cycles[23]. In agreement with our previous results[6,27,28], the formulations based on ABZ and P188 presented both *in-vitro* and *in-vivo* improved performances, thus P188 was selected as the stabilizer for further studies.

ABZ suspensions with increasing P188 concentrations (0.25, 0.5, 1 and 2.5%; NS_{4-7} respectively) were processed at 20 cycles of 1000 and 1200 bar, see Figure 2. Variations in the stabilizer concentration did not influence the final particle size, but an increase in the homogenization pressure produced a corresponding decrease in particle size, with a difference of ~150 nm being observed between nanosuspensions processed at 1000 and 1200 bar.

The presence of particles above the submicron range can produce physical destabilization by Ostwald ripening[29]. Theoretically, the increase in drug surface area leads to an increase in Gibbs free energy. Thus, the system prefers to reduce this increase by agglomeration, leading to particle size increase and poor stability[30]. Although ABZ nanocrystal suspensions were designed to be immediately dried and transformed into solid/redispersible powders, the particle size and PI were evaluated for 7 days to discard any eventual physical instability. As observed in Figure 3, NS_{4-7} containing P188 at 0.25, 0.5, 1 and 2.5%, respectively, remained stable for at least five days. Although some oscillations were observed on day 7, all the samples were easily redispersed before measurement and remained in the submicron range throughout the test.

Spray-drying process and particle redispersion

Spray-drying converts a liquid into a powder in one-step process. The operating conditions in SD must be carefully selected in order to obtain a high process yield and also to protect against possible thermal decomposition of the actives/excipients. In our SD experiment the combination of certain factors, such as a low inlet temperature (45 °C), high atomization air flow rate (819 l/h) and low

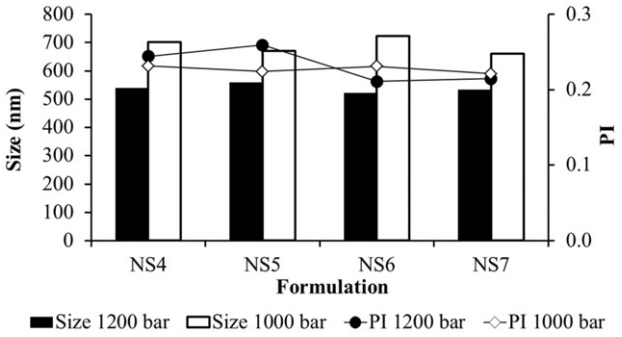

Figure 2. Effect of homogenization pressure (1000 and 1200 bar) and P188 concentration on final particle size and PI.

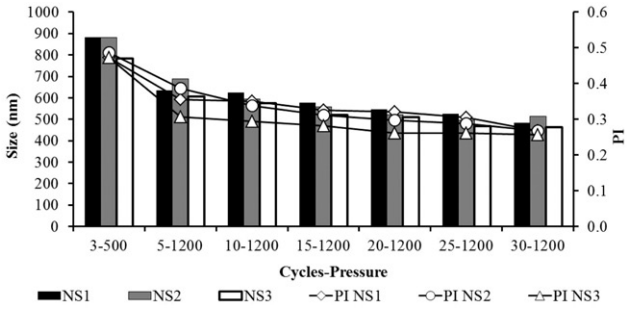

Figure 1. Reduction in particle size and PI with increasing homogenization cycles at 1200 bar for three stabilizer formulations: Poloxamer 188, Poloxamer 407 and SDS (NS1, NS2 and NS3, respectively)

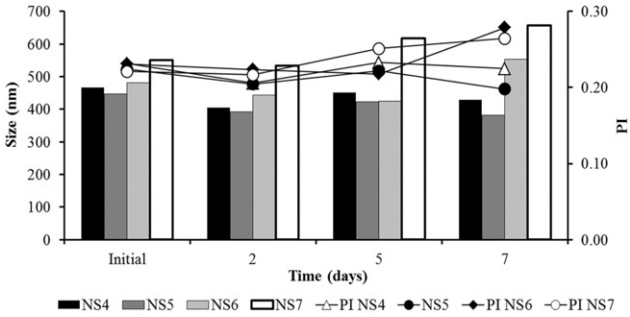

Figure 3. Influence of P188 concentration on particle aggregation at room temperature.

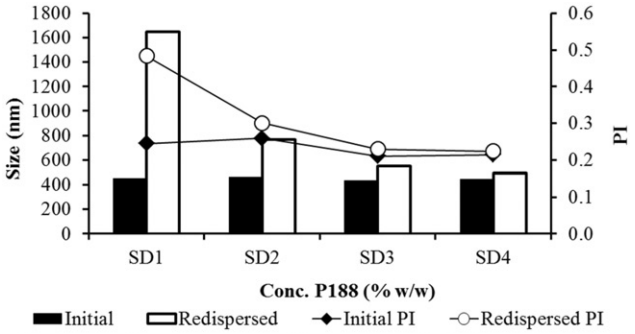

Figure 4. Nanocrystal redispersability of spray-dried powders at different concentrations of P188.

Table 3. Process yield of SD formulations and particle size of redispersed powders. SD_{1-4} were obtained from NS_{4-7} respectively. SD_5 and SD_6 were obtained from NS_7 by varying the amount of lactose.

Formulation	Yield (%)	Redispersion Size (nm)	Moisture content (%)
Before Drying	–	492.80 ± 7.90	–
SD_1	<10	1648.00 ± 135.23	2.21
SD_2	<10	769.53 ± 33.32	1.96
SD_3	21.28	563.53 ± 12.05	1.83
SD_4	70.20	550.60 ± 8.93	2.20
SD_5	74.32	552.97 ± 8.31	1.74
SD_6	60.13	548.40 ± 17.38	1.91

feed velocity (2 ml/min), allowed a high specific surface of the atomized nanosuspensions to be obtained. Therefore, it was possible to successfully remove water from the droplets as well as to impede P188 from reaching its melting point (52–57 °C), which produced high adhesion to the cyclone separator, and ergo very low process yields, as we observed in previous studies at higher inlet temperatures (data not shown).

The spray-dried formulations SD_1–SD_4 which had increasing concentrations of P188 (0.25, 0.5, 1 and 2.5% respectively), showed a clear tendency to improve particle redispersion and process yield. When a nanosuspension is atomized in a two-fluid nozzle, an abrupt increase in kinetic energy and shear force takes place and at this point the crystals in the nanosuspension may collide with each other if their velocity is high enough. This particle collision can partially damage the surfactant film which coats the interface, producing irreversible particle aggregation[31]. This is in agreement with the data shown in Figure 4, with SD_4 showing a similar particle size and PI (~490 nm and 0.224, respectively) as its original nanosuspension NS_7 (~450 nm and 0.215, respectively), whereas a difference of 1200 nm was observed when SD_1 was compared to NS_4 (0.25% P188). On the other hand, lower process yields at decreasing P188 concentrations might be attributed to the lack of separation efficiency in the cyclone. Formulations with smaller P188 proportions, which imply fewer solids in the droplet, will form smaller particles that are easily removed by the gas stream[31]. As shown in Table 3, SD_4 presented a 70.2% yield, while SD_1 and

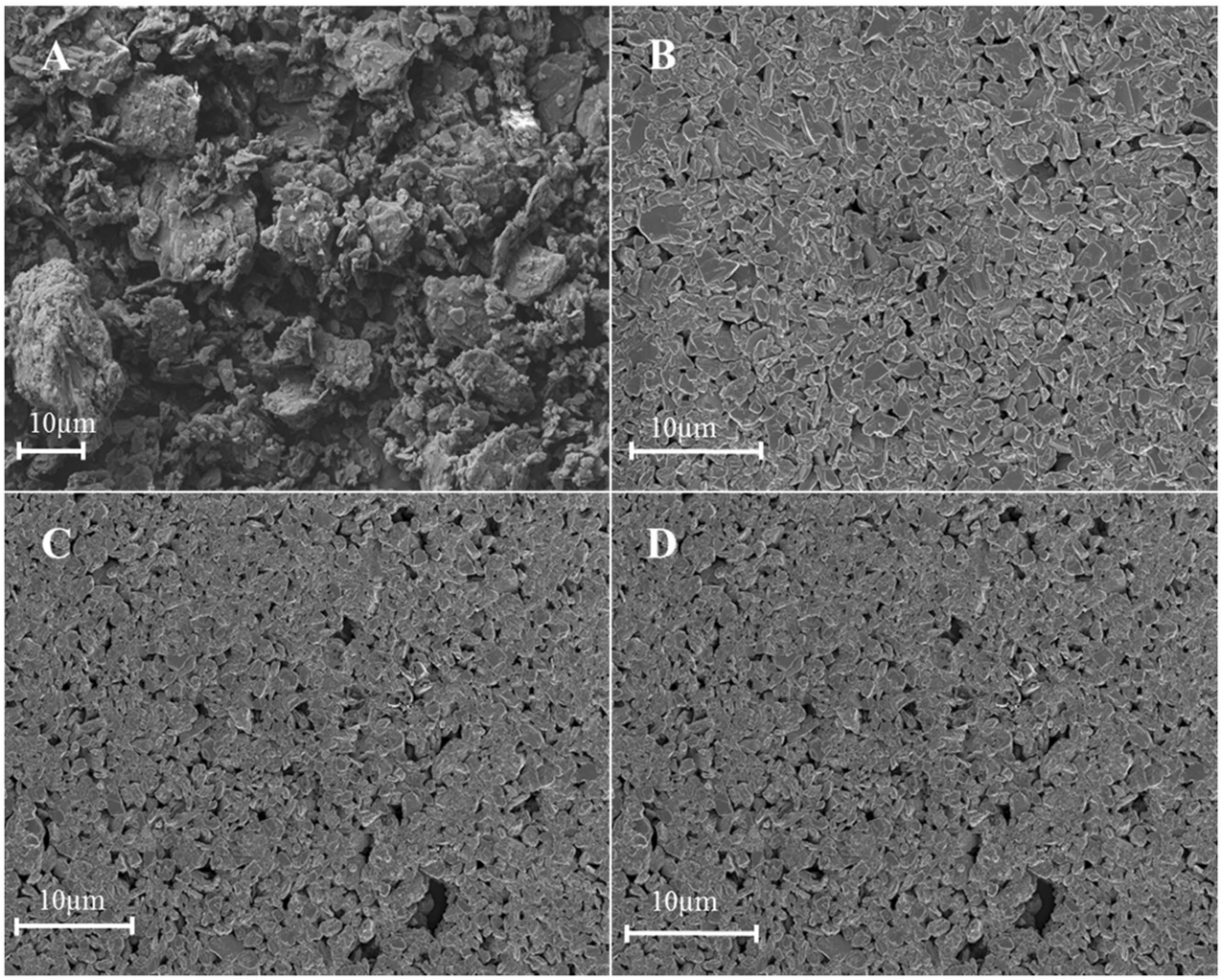

Figure 5. SEM micrographs of (A) pure ABZ, (B) homogenized nanosuspension NS7, (C) spray-dried powder SD4 and (D) redispersed nanocrystals (SD4).

SD_2 did not exceed 10%. Although a high moisture content in the sprayed droplet might cause adhesion to the cyclone, this phenomenon was discarded since the amount of humidity was approximately 2% for all SD samples.

The formulations SD_4, SD_5 and SD_6 contained different lactose:ABZ ratios (1:6, 1:3 and 0, respectively), with addition of an excess of lactose (i.e. SD_5, 1:3 ratio, yield 74.32%) appearing to improve the process performance whereas the absence of this material made the process less efficient (i.e. SD_6, without lactose, yield 60.13%). Although extensive studies were not performed, it can be hypothesized that lactose influences critical powder properties, such as the glass transition temperature (T_g). However, with the aim of optimizing the formulation weight/size, SD_4 (1:6 ratio, yield 70.20%) was chosen to continue the study.

Microscopy

Scanning electron microscopy micrographs (Figure 5) revealed large differences in particle size and shape between pure ABZ (Figure 5A) and processed materials in Figure 5(B, C and D) (NS_7, powdered SD_4 and redispersed SD_4, respectively). In addition, it can be seen that both the ABZ nanosuspension (Figure 5B) and

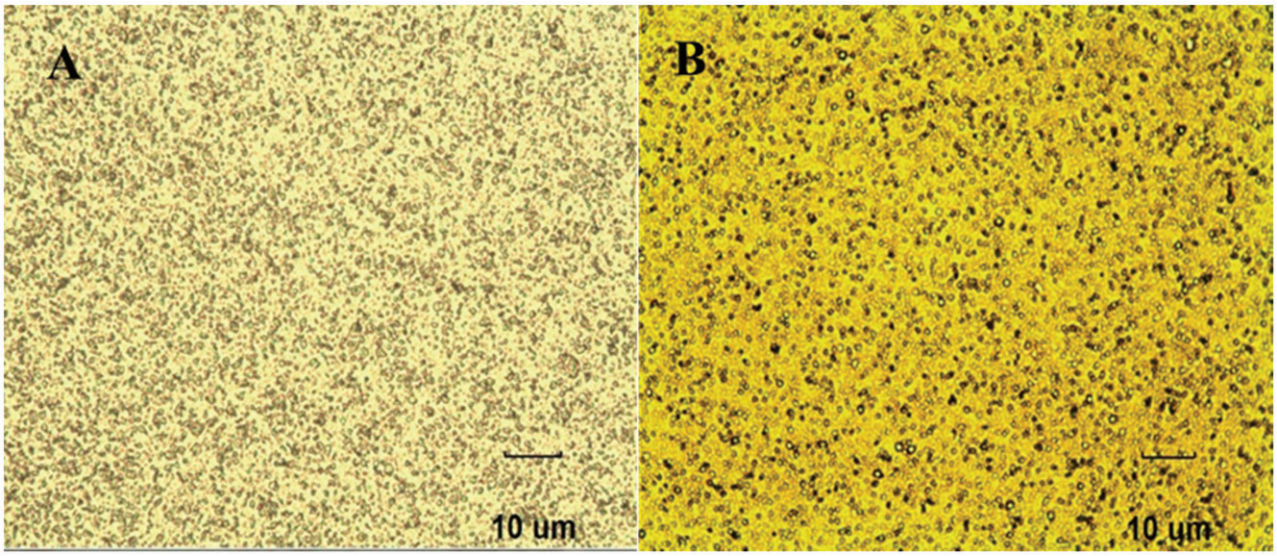

Figure 6. Micrographs from optical microscopy of nanosuspension NS7 (A) and redispersed powder SD4 (B).

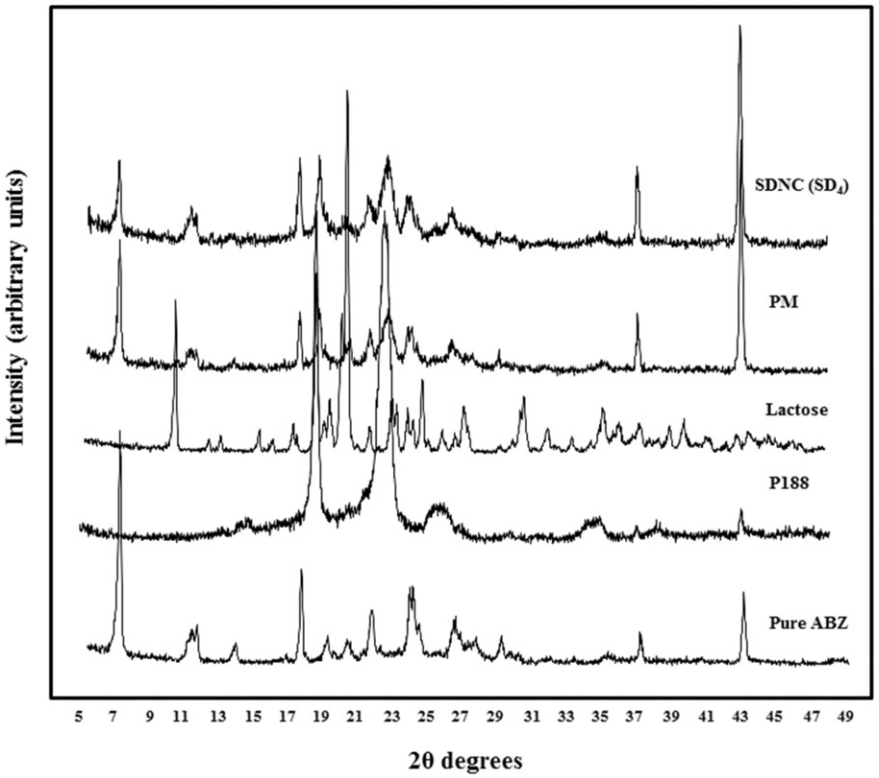

Figure 7. X-ray diffraction patterns of excipients lactose, P188, Pure ABZ, Physical Mixture and SDNCs SD4.

Table 4. Solubility of ABZ, physical mixture (PM) and SDNC (SD_4) in water and HCl 0.1N.

Solubilization medium	ABZ	PM	SDNCs
Water ($mg.l^{-1}$)	5.18 ± 1.02	5.18 ± 1.02	20.85 ± 2.81
HCl 0.1N ($mg.l^{-1}$)	420.04 ± 28.85	412.94 ± 32.65	609.26 ± 65.17

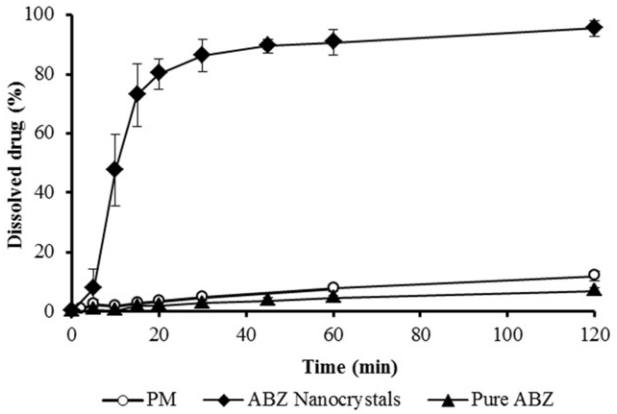

Figure 8. Dissolution data of pure ABZ, Physical Mixture and SDNCs (SD4). HCl 0.1 N at 37 °C, Method 1 USP at 75 rpm.

the spray-dried powder (Figure 5C) presented a high uniformity of particle size and were within the submicron range. On the other hand, these two samples did not show any marked differences in morphology, since both presented particles with a flake shape.

As described above, the key features of nanocrystals are directly linked to an increased contact surface, especially below the submicron range. Optical microscopy was used to demonstrate the absence of particle aggregates in the nanosuspension NS_7 (Figure 6A) or the redispersed powder SD_4 (Figure 6B). As observed in Figure 6, both samples showed no detectable particle clusters.

PXRD

It is known that milling can cause morphological changes, such as amorphization and polymorph transformation, with these phenomena often being attributed to the high input of mechanical energy caused by milling[32]. Although HPH is a high energy process able to produce changes in the crystalline pattern of drugs, the characteristic peaks of ABZ (7, 37 and 43 2θ degrees) are clearly observed in Figure 7 for both pure ABZ and ABZ SDNC, thus confirming that HPH and SD had no influence on the ABZ crystalline state.

Solubility assay

As shown in Table 4, the solubility of ABZ and PM showed no significant differences independent of the solubilization media, water and HCl 0.1N. In this way, the effect of P188 on ABZ solubility was practically negligible regarding the PM. According to the Noyes-Whitney equation[23,33], the enlarged specific surface of ABZ SDNC (SD_4) allowed greatly enhanced saturation concentrations to be obtained in water and HCl 0.1N (400 and 140%, respectively) when compared to pure ABZ or PM.

Dissolution study

The dissolution assay permits the behavior of a formulation to be understood when administered orally. As observed in Figure 8, ABZ dissolution from the SDNC seemed to be substantially faster than that from pure ABZ or the PM. For the former, a short lag time was observed (about 5 min), possibly being attributed to the release delay of SDNC from the capsules. However, this effect was practically negligible owing to the very fast dispersion of nanocrystals once they were in contact with the aqueous media.

For ABZ SDNC, a dissolution rate of approximately 80% at 20 min was observed, while for pure ABZ and its PM with P188 the dissolution rates were lower than 10% at 120 min. The large surface area of SDNC, in addition to the wetting effect of P188, appeared to be the main reasons this effect was produced. It is worth pointing out that the concentration of the surfactant was high enough to exert its wetting effect, but not sufficient to delay drug release due to its thermal gelation ability, as we were able to verify previously[27,28]. It is well known that for class II drugs an increase in dissolution rate and solubility leads to improved/predictable pharmacokinetic performances and probably requires a dosage adjustment.

Conclusions

Self-dispersable ABZ nanocrystal powder was obtained by HPH followed by SD. The main variables influencing both processes were studied, with homogenization pressure and stabilizer concentration found to be critical parameters for HPH and SD, respectively, and which had a great impact on important properties, such as redispersion and process yield. ABZ SDNC with a final particle size of approximately 500 nm were able to improve the pure ABZ physicochemical properties, such as saturation concentration and dissolution rate, with no variations in X-ray patterns being observed in ABZ SDNC samples when compared with the pure ABZ control.

The process developed is a simple and fast approach to produce ABZ nanocrystals in a water-redispersible powder form. These results demonstrate the potential of coupling HPH and SD to achieve a novel product with an improved dissolution rate.

Acknowledgements

The authors wish to acknowledge RUMAPEL, Argentina for having kindly donated the Poloxamer 407 and 188. Dr Paul Hobson (native speaker) revised the final version of the manuscript.

Disclosure statement

The authors report no declarations of interest. The present work was performed with the assistance of the Consejo Nacional de Investigaciones Científicas y Técnicas (CONICET), SECyT-UNC, Universidad Nacional de Córdoba and Universidad Nacional del Centro de la Provincia de Buenos Aires. Alejandro Javier Paredes is a CONICET PhD fellow.

References

1. Lacey E. Mode of action of benzimidazoles. Parasitol Today 1990;6:112–15.
2. Pensel PE, Castro S, Allemandi D, et al. Enhanced chemoprophylactic and clinical efficacy of albendazole formulated as solid dispersions in experimental cystic echinococcosis. Vet Parasitol 2014;203:80–6.
3. Amidon GL, Lennernäs H, Shah VP, Crison JR. A theoretical basis for a biopharmaceutic drug classification: the correlation of in vitro drug product dissolution and in vivo bioavailability. Pharmaceut Res 1995;3:413–20.

4. Jung H, Medina L, García L, Fuentes IM-ER. Absorption studies of albendazole and some physicochemical properties of the drug and its metabolite albendazole sulphoxide. J Pharm Pharmacol 1998;1:43–8.
5. Daniel-Mwambete K, Torrado S, Cuesta-Bandera C, et al. The effect of solubilization on the oral bioavailability of three benzimidazole carbamate drugs. Int J Pharm 2004;272:29–36.
6. Castro SG, Sanchez Bruni SF, Urbizu LP, et al. Enhanced dissolution and systemic availability of albendazole formulated as solid dispersions. Pharm Dev Technol 2012;18:1–9.
7. Shuhua X, Jiqing Y, Mingjie W, et al. Augmented bioavailability and cysticidal activity of albendazole reformulated in soybean emulsion in mice infected with *Echinococcus granulosus* or *Echinococcus multilocularis*. Acta Trop 2002;82:77–84.
8. Wen H, New RR, Muhmut M, et al. Pharmacology and efficacy of liposome-entrapped albendazole in experimental secondary alveolar echinococcosis and effect of co-administration with cimetidine. Parasitology 1996;113:111–21.
9. Kata M, Schauer M. Increasing the solubility characteristics of albendazole with dimethyl-beta-cyclodextrin. Acta Pharm Hung 1991;61:23–31.
10. Vogt M, Kunath K, Dressman JB. Dissolution improvement of four poorly water soluble drugs by cogrinding with commonly used excipients. Eur J Pharm Biopharm 2008;68:330–7.
11. Palomares-Alonso F, Jung-Cook H, Pérez-Villanueva J, et al. Synthesis and in vitro cysticidal activity of new benzimidazole derivatives. Eur J Med Chem 2009;44:1794–800.
12. Rivera JC, Yépez-Mulia L, Hernández-Campos A, et al. Biopharmaceutic evaluation of novel anthelmintic (1H-benzimidazol-5(6)-yl)carboxamide derivatives. Int J Pharm 2007;343:159–65.
13. Lange H, Eggers R, Bircher J. Increased systemic availability of albendazole when taken with a fatty meal. Eur J Clin Pharmacol 1988;34:315–17.
14. Nagy J, Schipper H, Koopmanns R, et al. Effect of grapefruit juice or cimetidine coadministration on albendazole bioavailability. Am J Trop Med Hyg 2002;66:260–3.
15. Torrado S, López ML, Torrado G, et al. A novel formulation of albendazole solution: oral bioavailability and efficacy evaluation. Int J Pharm 1997;156:181–7.
16. del Estal JL, Alvarez AI, Villaverde C, et al. Increased systemic bioavailability of albendazol when administered with surfactants in rats. Int J Pharm 1994;102:257–60.
17. Mingjie W, Shuhua X, Junjie C, et al. Albendazole–soybean oil emulsion for the treatment of human cystic echinococcosis: evaluation of bioavailability and bioequivalence. Acta Trop 2002;83:177–81.
18. García JJ, Bolás F, Torrado JJ. Bioavailability and efficacy characteristics of two different oral liquid formulations of albendazole. Int J Pharm 2003;250:351–8.
19. Ceballos L, Elissondo C, Moreno L, et al. Albendazole treatment in cystic echinococcosis: pharmacokinetics and clinical efficacy of two different aqueous formulations. Parasitol Res 2008;103:355–62.
20. Ceballos L, Elissondo M, Bruni SS, et al. Flubendazole in cystic echinococcosis therapy: pharmaco-parasitological evaluation in mice. Parasitol Int 2009;58:354–8.
21. Ceballos L, Elissondo C, Sánchez Bruni S, et al. Chemoprophylactic activity of flubendazole in cystic echinococcosis. Chemotherapy 2010;56:386–92.
22. Liu C, Zhang H, Jiang B, et al. Enhanced bioavailability and cysticidal effect of three mebendazole-oil preparations in mice infected with secondary cysts of *Echinococcus granulosus*. Parasitol Res 2012;111:1205–11.
23. Keck CM, Müller RH. Drug nanocrystals of poorly soluble drugs produced by high pressure homogenisation. Eur J Pharm Biopharm 2006;62:3–16.
24. Noyes AA, Whitney WR. The rate of solution of solid substances in their own solutions. J Am Chem Soc 1897;19:930–4.
25. Raghava Srivalli KM, Mishra B. Drug nanocrystals: a way toward scale-up. Saudi Pharm J. 2016. [Epub ahead of print]. doi:10.1016/j.jsps.2014.04.007.
26. Zuo B, Sun Y, Li H, et al. Preparation and in vitro/in vivo evaluation of fenofibrate nanocrystals. Int J Pharm 2013;455:267–75.
27. Castro S, Bruni S, Lanusse C, et al. Improved albendazole dissolution rate in pluronic 188 solid dispersions. AAPS Pharm Sci Tech 2010;11:1518–25.
28. Dib A, Palma S, Suárez G, et al. Albendazole sulphoxide kinetic disposition after treatment with different formulations in dogs. J Vet Pharmacol Ther 2011;34:136–41.
29. Keck CM. Particle size analysis of nanocrystals: improved analysis method. Int J Pharm 2010;390:3–12.
30. Sun W, Tian W, Zhang Y, et al. Effect of novel stabilizers-cationic polymers on the particle size and physical stability of poorly soluble drug nanocrystals. Nanomed Nanotechnol Biol Med. 2012;8:460–7.
31. Freitas C, Müller RH. Spray-drying of solid lipid nanoparticles (SLNTM). Eur J Pharm Biopharm 1998;46:145–51.
32. Kluge J, Muhrer G, Mazzotti M. High pressure homogenization of pharmaceutical solids. J Supercrit Fluids 2012;66:380–8.
33. Mauludin R, Müller RH, Keck CM. Development of an oral rutin nanocrystal formulation. Int J Pharm 2009;370:202–9.